

## RESEARCH ARTICLE

# A three-range approach enhances the prognostic utility of CSF biomarkers in Alzheimer's disease

Wagner S. Brum<sup>1,2</sup> | Marco Antônio de Bastiani<sup>1</sup> | Andrei Bieger<sup>1</sup> | Joseph Therriault<sup>3,4</sup> | João P. Ferrari-Souza<sup>1,12</sup> | Andréa L. Benedet<sup>2,3,4</sup> | Paramita Saha-Chaudhuri<sup>5</sup> | Diogo O. Souza<sup>1,6</sup> | Nicholas J. Ashton<sup>2,7,8</sup> | Henrik Zetterberg<sup>2,9,10,11</sup> | Tharick A. Pascoal<sup>12</sup> | Thomas Karikari<sup>2,12</sup> | Kaj Blennow<sup>2,9</sup> | Pedro Rosa-Neto<sup>3,4</sup> | Eduardo R. Zimmer<sup>1,13,14</sup> | Alzheimer's Disease Neuroimaging Initiative (ADNI)

<sup>1</sup> Graduate Program in Biological Sciences: Biochemistry, Universidade Federal do Rio Grande do Sul (UFRGS), Porto Alegre, Brazil

<sup>2</sup> Department of Psychiatry and Neurochemistry, The Sahlgrenska Academy at the University of Gothenburg, Mölndal, Sweden

<sup>3</sup> Translational Neuroimaging Laboratory, The McGill University Research Centre for Studies in Aging, LaSalle Boulevard, Verdun, Canada

<sup>4</sup> Department of Neurology and Neurosurgery, McGill University, Montreal, Canada

<sup>5</sup> Department of Mathematics and Statistics, University of Vermont, Burlington, USA

<sup>6</sup> Department of Biochemistry, UFRGS, Porto Alegre, Brazil

<sup>7</sup> Department of Old Age Psychiatry, Institute of Psychiatry, Psychology & Neuroscience, King's College London, London, UK

<sup>8</sup> Wallenberg Centre for Molecular and Translational Medicine, University of Gothenburg, Gothenburg, Sweden

<sup>9</sup> Clinical Neurochemistry Laboratory, Sahlgrenska University Hospital, Gothenburg, Sweden

<sup>10</sup> Department of Neurodegenerative Disease, UCL Queen Square Institute of Neurology, London, UK

<sup>11</sup> UK Dementia Research Institute at UCL, London, UK

<sup>12</sup> Department of Neurology and Psychiatry, University of Pittsburgh, Pittsburgh, USA

<sup>13</sup> Department of Pharmacology, UFRGS, Porto Alegre, Brazil

<sup>14</sup> Graduate Program in Biological Sciences: Pharmacology and Therapeutics, UFRGS, Porto Alegre, Brazil

## Correspondence

Eduardo R. Zimmer, Department of Pharmacology, UFRGS, Rua Ramiro Barcelos, 2600, Porto Alegre, Brazil.

Email: [eduardo.zimmer@ufrgs.br](mailto:eduardo.zimmer@ufrgs.br)

## Funding information

CAPES, Grant/Award Numbers: 88887.372371/2019-00, 88887.596742/2020-00; CNPq, Grant/Award Numbers: 150293/2019-4, 88882.345554/2019-01, 88887.518039/2020-00; CNPq/INCT, Grant/Award Number: 465671/2014-4; CNPq/ZIKA, Grant/Award Number:

## Abstract

**Introduction:** Alzheimer's disease consensus recommends biomarker dichotomization, a practice with well-described clinical strengths and methodological limitations. Although neuroimaging studies have explored alternative biomarker interpretation strategies, a formally defined three-range approach and its prognostic impact remains under-explored for cerebrospinal fluid (CSF) biomarkers.

**Methods:** With two-graph receiver-operating characteristics based on different reference schemes, we derived three-range cut-points for CSF Elecsys biomarkers. According to baseline CSF status, we assessed the prognostic utility of this in predicting risk of clinical progression and longitudinal trajectories of cognitive decline and amyloid-

This is an open access article under the terms of the [Creative Commons Attribution-NonCommercial-NoDerivs](https://creativecommons.org/licenses/by-nc-nd/4.0/) License, which permits use and distribution in any medium, provided the original work is properly cited, the use is non-commercial and no modifications or adaptations are made.

© 2022 The Authors. *Alzheimer's & Dementia: Diagnosis, Assessment & Disease Monitoring* published by Wiley Periodicals, LLC on behalf of Alzheimer's Association

440763/2016-9; CNPq/FAPERGS/PRONEX, Grant/Award Numbers: 16/2551-0000475-7, 19/2551-0000700-0, 88887.507218/2020-00, 88887.507161/2020-00, #2018-02532; European Research Council, Grant/Award Number: #681712; Swedish State Support for Clinical Research, Grant/Award Number: #ALFGBG-720931; Alzheimer Drug Discovery Foundation, Grant/Award Number: #201809-2016862; AD Strategic Fund; the Alzheimer's Association, Grant/Award Numbers: #ADSF-21-831376-C, #ADSF-21-831381-C, #ADSF-21-831377-C, #AARGD-21-850670; the Olav Thon Foundation; the Erling-Persson Family Foundation; Stiftelsen för Gamla Tjänarinnor, Hjärtfonden, Grant/Award Number: #FO2019-0228; European Union's Horizon 2020; the Marie Skłodowska-Curie, Grant/Award Numbers: 860197, UK Dementia Research Institute; BrightFocus Foundation, Grant/Award Number: #A2020812F; Neurochemistry's Career Development Grant; the Swedish Alzheimer Foundation, Grant/Award Number: #AF-930627; the Swedish Brain Foundation, Grant/Award Number: #FO2020-0240; the Swedish Dementia Foundation; the Swedish Parkinson Foundation; Gamla Tjänarinnor Foundation; the Aina; Wallströms and Mary-Ann Sjöbloms Foundation; Agneta Prytz-Folkes & Gösta Folkes Foundation, Grant/Award Number: #2020-00124; the Gun and Bertil Stohnes Foundation; the Anna Lisa and Brother Björnsson's Foundation; the Swedish Research Council, Grant/Award Numbers: #2017-00915, #RDAPB-201809-2016615, #AF-742881, #ALFGBG-715986; European Union Joint Program for Neurodegenerative Disorders, Grant/Award Number: JPN2019-466-236; National Institutes of Health (NIH), Grant/Award Number: #1R01AG068398-01; McGill University Faculty of Medicine; Alzheimer's Society of Canada; Weston Brain Institute, and Canadian Institutes of Health Research, Grant/Award Numbers: 435642/2018-9, 312410/2018-2; Instituto Serrapilheira, Grant/Award Number: Serra-1912-31365; Brazilian National Institute of Science and Technology in Excitotoxicity and Neuroprotection, Grant/Award Number: 465671/2014-4; FAPERGS/MS/CNPq/SESRS-PPSUS, Grant/Award Number: 30786.434.24734.23112017; ARD/FAPERGS, Grant/Award Number: 21/2551-0000673-0

beta ( $A\beta$ ) positron emission tomography (PET) accumulation in non-demented individuals (Alzheimer's Disease Neuroimaging Initiative [ADNI];  $n = 1246$ ). In all analyses, we compared herein-derived three-range CSF cut-points to previously described binary ones.

**Results:** In our main longitudinal analyses, we highlight CSF  $p\text{-tau}_{181}/A\beta_{1-42}$  three-range cut-points derived based on the cognitively normal  $A\beta$ -PET negative versus dementia  $A\beta$ -PET positive reference scheme for best depicting a prognostically relevant biomarker abnormality range. Longitudinally, our approach revealed a divergent intermediate cognitive trajectory undetected by dichotomization and a clearly abnormal group at higher risk for cognitive decline, with power analyses suggesting the latter group as potential trial enrichment candidates. Furthermore, we demonstrate that individuals with intermediate-range CSF status have similar rates of  $A\beta$  deposition to those in the clearly abnormal group.

**Discussion:** The proposed approach can refine clinico-biological prognostic assessment and potentially enhance trial recruitment, as it captures faster biomarker-related cognitive decline in comparison to binary cut-points. Although this approach has implications for trial recruitment and observational studies, further discussion is needed regarding clinical practice applications.

#### KEYWORDS

Alzheimer's disease, CSF biomarkers, cut-points, prognostic modeling, three-range

## 1 | INTRODUCTION

In 2018, a National Institute on Aging–Alzheimer's Association (NIA-AA) working group developed a Research Framework to biologically define Alzheimer's disease (AD).<sup>1</sup> Similarly to previous clinico-biological criteria,<sup>2,3</sup> the Research Framework recommends dichotomization of AD biomarkers, that is, the use of normal/abnormal status based on a single threshold to define biomarker profiles for amyloid, tau, and neurodegeneration, proposing the AT(N) system.<sup>1</sup>

Although this practical approach has enabled systematic characterization of AD's preclinical phase<sup>2,3</sup> and facilitated recruitment for clinical trials of disease-modifying therapies,<sup>4,5</sup> the NIA-AA Research Framework acknowledges that dichotomization is context dependent and that continuous-variable modeling might be more appropriate for many studies.<sup>1</sup> In fact, it also suggests that a three-range approach might also be a useful strategy in AD research.

Recently, limitations of the dichotomous classification have been in the spotlight. In a perspective article, McRae-McKee and colleagues<sup>6</sup>

elaborated that the “gray zone” around a binary threshold should be taken into consideration for a more reliable prognostic assessment. Concerning practical alternatives, neuroimaging research studies suggested that a three-range approach can better stratify prognostic assessment<sup>7,8</sup> and refine stratification of amyloid- $\beta$  ( $A\beta$ ) positron emission tomography (PET) accumulation trajectories.<sup>7</sup> Although the importance of intermediate values has been highlighted for cerebrospinal fluid (CSF) biomarkers and amyloid-PET agreement,<sup>9</sup> it remains unclear whether a three-range approach for CSF biomarkers might also lead to improved prognostic prediction of relevant clinico-biological features.

Biological outcomes have gained attention in AD drug trials; however, the main goal is still to slow the progression of clinical symptoms.<sup>10</sup> In this regard, with several trials adopting CSF abnormality as enrollment criteria,<sup>4</sup> an improved risk stratification could benefit the recruitment from a cost-effectiveness perspective, so that individuals with a higher risk of AD-related cognitive decline are enrolled. Beyond trials, starting the discussion on dichotomization alternatives within the AD fluid biomarkers field of observational research is much needed to enable future clinical applications.

Here, we derived three-range cut-points for CSF biomarkers with two-graph receiver-operating characteristics (TG-ROC) and investigated their prognostic value for predicting cognitive decline, clinical progression, and amyloid accumulation in non-demented individuals, highlighting their application to the phosphorylated tau/ $A\beta_{1-42}$  (p-tau<sub>181</sub>/ $A\beta_{1-42}$ ) ratio. Because continuous biomarkers generally have a continuous relationship with clinical outcomes,<sup>11</sup> we hypothesized that a three-range approach for interpreting CSF biomarkers would reveal an intermediate-risk category undetected by dichotomously handling the same measurements.

## 2 | METHODS

### 2.1 | Participants and study design

We used data from the Alzheimer's Disease Neuroimaging Initiative (ADNI; NCT00106899; <http://adni.loni.usc.edu/>), a study approved by all participating institutional review boards. Informed consent was provided by the participants or their authorized representatives. Specific protocols and enrollment criteria for the ADNI<sup>12</sup> have been described elsewhere.

We derived three-range cut-points in a subset of ADNI participants with available CSF Elecsys biomarker measurements and [<sup>18</sup>F]-florbetapir amyloid-PET (cognitively unimpaired [CU],  $n = 361$ ; mild cognitive impairment [MCI],  $n = 474$ ; dementia,  $n = 157$ ). Then, cut-points were evaluated in our main longitudinal set of ADNI participants, consisting of individuals without dementia and available CSF Elecsys biomarkers (CU,  $n = 562$ ; MCI,  $n = 684$ ). First, we evaluated cross-sectional associations of the three-range CSF approach with baseline cognition and [<sup>18</sup>F]-florbetapir levels (individuals with matched baseline CSF and [<sup>18</sup>F]-florbetapir: CU,  $n = 342$ ; MCI,  $n = 475$ ). Since our main goal was to assess the prognostic relevance

### RESEARCH IN CONTEXT

- 1. Systematic review:** We reviewed the literature using PubMed and conference abstracts. Dichotomous classification of Alzheimer's disease (AD) biomarkers has gained importance with the publication of the National Institute on Aging–Alzheimer's Association (NIA-AA) Research Framework, and potential limitations of this practice were recently discussed in this journal. In this context, alternative strategies for interpreting cerebrospinal fluid (CSF) biomarkers remain underexplored. Therefore, we aimed to operationalize three-range cut-points—using two-graph receiver-operating characteristics (TG-ROC)—for CSF AD biomarkers and to focus on their prognostic utility.
- 2. Interpretation:** Longitudinally, this approach reveals an intermediate cognitive trajectory undetected by binary cut-points and a faster declining clearly abnormal group. In addition, this approach identified that individuals with intermediate biomarker levels experience similar rates of amyloid- $\beta$  accumulation to those with clearly abnormal levels. These findings highlight that three-range cut-points may enhance clinico-biological prognostic assessment, with potential applications to clinical trial recruitment.
- 3. Future directions:** This study had the goal of investigating the prognostic utility of the novel approach. Further research is needed to elaborate alternative interpretation strategies in a clinical decision-making context, as well as for other AD fluid biomarker modalities.

of three-range cut-points based on baseline CSF biomarkers, we evaluated their impact over longitudinal cognitive trajectories and risk of clinical progression over 6 years. For those individuals containing matched baseline CSF and amyloid-PET with available follow-up visits, we evaluated [<sup>18</sup>F]-florbetapir longitudinal trajectories over 4 years. (See Figure S1 for a schematic illustration of study design.)

### 2.2 | CSF biomarkers

CSF  $A\beta_{1-42}$ , p-tau<sub>181</sub>, and total tau (t-tau) were measured using the validated fully automated Elecsys immunoassay (Roche Diagnostics GmbH, Penzberg, Germany).<sup>13,14</sup> Measurements outside the analytical range were handled as described in the Supplement.<sup>15,16</sup> For comparability, previously described<sup>15</sup> binary cut-points were used: <976.6 pg/mL for  $A\beta_{1-42}$ , >24 pg/mL for p-tau<sub>181</sub>, >266 pg/mL for t-tau, >0.0251 for the p-tau<sub>181</sub>/ $A\beta_{1-42}$  ratio, and >0.27 for the t-tau/ $A\beta_{1-42}$  ratio.

## 2.3 | Statistical analyses

All analyses were performed using R Statistical Software ([www.r-project.org](http://www.r-project.org))<sup>17–23</sup> and are described in the following sections. Statistical significance was set as  $\alpha = 0.05$ .

### 2.3.1 | Outcomes

For cross-sectional and longitudinal analyses of cognition, we used the Preclinical Alzheimer's Cognitive Composite (mPACC)<sup>24</sup> in its modified version including Trail Making Test B. For time-to-event analyses, outcomes were the progression from a baseline CU diagnosis to MCI or from a baseline MCI diagnosis to dementia.<sup>12</sup> For assessing longitudinal amyloid PET deposition, we used the [<sup>18</sup>F]-florbetapir global standardized uptake value ratio (SUVR) normalized by subcortical eroded white matter, recommended for this purpose.<sup>25</sup>

### 2.3.2 | Cut-point derivation

For deriving three-range cut-points, we performed two-graph receiver operating characteristics (or TG-ROC).<sup>26</sup> Instead of dichotomously aiming for the best trade-off between sensitivity and specificity, TG-ROC defines two cut-points: a lower cut-point, based on test values with 90% specificity, and an upper cut-point, based on values with 90% sensitivity.

For each evaluated CSF biomarker, we performed TG-ROC analyses with 1000 bootstraps for three different reference schemes: (1) amyloid-PET negative versus amyloid-PET positive; (2) CU amyloid-PET negative versus cognitively impaired (CI) amyloid-PET positive; (3) CU amyloid-PET negative versus dementia amyloid-PET positive. Although for diagnostic purposes CSF  $A\beta_{1-42}$  cut-points are usually better derived when contrasting  $A\beta-$  to  $A\beta+$  groups (scheme i), there is an open discussion for tau and tau/ $A\beta$  ratios, since contrasting CU  $A\beta-$  to impaired  $A\beta+$  groups (schemes ii and iii) might better capture tau-related abnormality in AD.<sup>16,27</sup> Thus, we included these reference groups, as such an abnormal range could be especially useful for prognostic assessment. To choose the biomarker and cut-point scheme combination for longitudinal analyses, we took into consideration the sensitivity of the lower and the specificity of the upper cut-point and, importantly, the clinical applicability of the cut-points, that is, if they covered an intermediate range wide enough to justify substituting binary cut-points.

### 2.3.3 | Mixed models

For all longitudinal analyses, four models were fitted using previously described binary and hereby-derived three-range cut-points: (1) CU at baseline, binary; (2) CU at baseline, three-range; (3) MCI at baseline, binary; and (4) MCI at baseline, three-range. Mean cognitive trajectories were estimated with linear mixed-effects (LME) models, including terms for biomarker status at baseline (binary or three-range), covariates (sex, apolipoprotein E (APOE)  $\epsilon 4$  status, age at baseline, years

of education) and their interactions with time<sup>28</sup>, to better account for potential effects of these covariates and to avoid effect overestimation of our group of interest. No three-way interactions were included. Within-participant correlation was accommodated by allowing for correlated random intercepts and slopes on time. We defined years since baseline as the time scale, with a 6-year follow-up period. Although our LME models had the main goal of comparing longitudinal trajectories between biomarker groups, baseline differences were also modeled.<sup>29,30</sup> Continuous predictors were centered, and variance inflation factors (VIFs) were calculated to evaluate the presence of multicollinearity. Within LME models, we compared the rates of cognitive decline between CSF biomarker groups based on a global evaluation of group-by-time interactions. Furthermore, we also compared binary and three-range models based on their  $R^2$  (a measure of how much the model explains outcome variability) and Akaike information criterion (AIC; a model goodness-of-fit measure). The same modeling strategy described above applies to mixed models evaluating longitudinal amyloid-PET deposition over 4 years.

### 2.3.4 | Time-to-event analyses

For time-to-event models, we included the following predictors: biomarker status at baseline (binary or three-range), sex, APOE  $\epsilon 4$  status, age, years of education, baseline mini-mental state examination (MMSE) and baseline Clinical Dementia Rating - Sum of Boxes (CDR-SB) scores. We compared estimated survival probabilities between group terms and carried generalized log-rank tests. (See Supplement for further information.)

### 2.3.5 | Power analyses

We performed clinical trial simulations to evaluate whether more stringent enrollment criteria for CSF biomarker abnormality could lead to power increases. We compared simulations using (1) the conventional binary cut-point to those (2) using the “clearly abnormal” participants (with “clearly normal” as the reference, ie, removing “intermediate range” participants from the simulations). With LME models ( $n = 1000$  bootstrap trials), we estimated the number of participants needed to detect, with 80% power, a 25% reduction in the rate of cognitive decline (measured with the mPACC), when compared to the biomarker-negative or “clearly normal” reference group. We specified clinical trial duration to be of 48 months for CU and 18 months for MCI individuals, with follow-up occurring every 3 months. Model specifications were based on previously described methodologies.<sup>31–34</sup>

## 3 | RESULTS

### 3.1 | Cut-point derivation

Among all reference groups and CSF biomarkers evaluated, the  $p$ -tau<sub>181</sub>/ $A\beta_{1-42}$  ratio cut-point pair of  $<0.0203$  and  $>0.0377$  not only

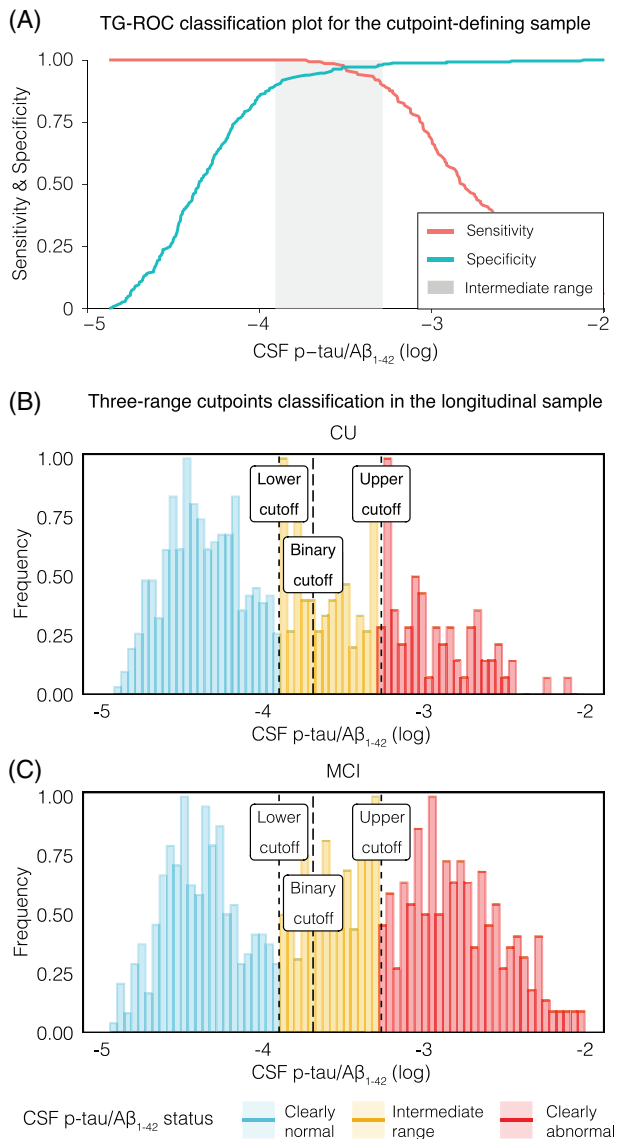


**FIGURE 1** The derivation of three-range cut-points and their application to the longitudinal sample. (A) Classification plot for CSF p-tau<sub>181</sub>/Aβ<sub>1-42</sub> two-graph receiver-operating characteristics (TG-ROC), derived within the cut-point defining the participant subset who had matched amyloid-PET scans and CSF biomarkers. The red line represents sensitivity and green line, specificity. To constitute the lower and upper cut-points (0.0203 and 0.0377), the biomarker values with 90% of sensitivity and 90% of specificity were selected, respectively. Measurements in-between these values are classified as being in the intermediate range, represented by the gray area. These metrics were obtained by assessing the biomarker's capacity for discriminating CU Aβ<sup>-</sup> from dementia Aβ<sup>+</sup> defined, with amyloid-PET. Metrics and plots based on other biomarkers and other reference schemes can be found in Figures S2 and S3; (B-C) Distribution of the longitudinal sample across CSF p-tau<sub>181</sub>/Aβ<sub>1-42</sub> three-range groups for the CU (B) and MCI (C) groups. It is shown that the derived intermediate range captures a range wide enough to justify expansion from a binary cut-point placed approximately in its center. Sample distributions based on the other biomarkers and cut-points are shown in Figure S3. CSF, cerebrospinal fluid; p-tau<sub>181</sub>, tau phosphorylated at threonine-181; Aβ<sub>1-42</sub>, amyloid beta 1-42; PET, positron emission tomography; CU, cognitively unimpaired; MCI, mild cognitive impairment

demonstrated the highest sensitivity for 90% specificity and highest specificity for 90% sensitivity when discriminating TG-ROC reference groups, but also best fit the criteria of providing a wide enough intermediate range that also encompassed the previously described binary cut-points. Furthermore, it had been previously described that the p-tau<sub>181</sub>/Aβ<sub>1-42</sub> ratio was prognostically superior to the other markers.<sup>15,16</sup> The t-tau/Aβ<sub>1-42</sub> ratio was not chosen, as this biomarker presents a nearly perfect overlap with p-tau,<sup>35</sup> when measured by the Elecsys assay. This specific chosen cut-point pair had CU amyloid-PET negative versus dementia amyloid-PET positive as the reference scheme. The classification plot for TG-ROC is shown in Figure 1A. Figures 1B and 1C display stratification of the main longitudinal subset of participants (CU, above; MCI; below) according to the derived cut-points. We used the NIA-AA Research Framework's terminology recommendations<sup>1</sup>: "clearly normal," "intermediate range," and "clearly abnormal."

Demographic information for the cut-point-defining sample is shown in Table S1. All derived cut-points, with their respective sensitivities and specificities, are described in Table S2 and Figure S2. Figure S3 demonstrates how the longitudinal sample would have been stratified, had we chosen other biomarkers and reference schemes.

### 3.2 | Demographic information and cross-sectional analyses

Demographic information for the longitudinal sample based on CSF p-tau<sub>181</sub>/Aβ<sub>1-42</sub> status is shown in Table 1. Overall, we observed similar relationships of key variables across the three-range abnormality spectrum, such as a decrease in cognitive scores and increases in age, proportion of cognitively impaired (CI) individuals, and proportion of APOE ε4 carriers. The median follow-up time was of 3.97 years.

Figures 2A and 2B show the continuous associations between CSF p-tau<sub>181</sub>/Aβ<sub>1-42</sub> levels and amyloid-PET, displaying CSF-PET correlation metrics for each three-range component. For CU individuals (Figure 2A), although the intermediate range encompassed the group-level ascending correlation slope, none of the three-range groups presented a statistically significant correlation. For MCI individuals (Figure 2B), the clearly normal ( $R = 0.27$ ,  $P < .001$ ) and intermediate range ( $R = 0.35$ ,  $P < .001$ ) groups presented statistically significant correlations between CSF p-tau<sub>181</sub>/Aβ<sub>1-42</sub> levels and amyloid-PET, whereas biomarker levels in the clearly abnormal group were not associated with amyloid-PET. Figure S4 demonstrates these associations for the other CSF biomarkers not included in the main text.

In Figure 2C-F, raincloud plots show differences in [<sup>18</sup>F]-florbetapir (expressed in centiloids [CLs]) across three-range or binary CSF p-tau<sub>181</sub>/Aβ<sub>1-42</sub> groups. The plots also include visual representations of where the usual amyloid-PET binary threshold lies, as well as of an amyloid-PET gray zone encompassing previously reported binary cut-points (12-35CL).<sup>25</sup> For CU individuals grouped with the binary cut-point (Figure 2C), biomarker-positive individuals have significantly ( $P < .001$ ) elevated amyloid-PET levels in contrast to biomarker-negative individuals. When stratifying CU individuals with the three-

**TABLE 1** Characteristics of the longitudinal sample by CSF p-tau<sub>181</sub>/Aβ<sub>1-42</sub> ratio three-range status

	Clearly normal	Intermediate range	Clearly abnormal
N, %	(650, 52.2)	(235, 18.8)	(361, 29.0)
Age, years, mean (SD)	71.2 (6.96)	74.3 (6.63)	74.0 (6.85)
Female, n (%)	327 (50.3)	119 (50.6)	160 (44.3)
APOE ε4 carriers, no (%)	131 (20.2)	118 (50.2)	256 (70.9)
Years of education, mean (SD)	16.5 (2.56)	16.1 (2.76)	16.1 (2.70)
Baseline cognitive status, n CU/MCI	384/266	116/119	105/256
Baseline MMSE score, mean (SD)	28.8 (1.35)	28.3 (1.71)	27.5 (1.96)
Baseline mPACC score, mean (SD)			
CU	0.263 (2.51)	−0.297 (2.63)	−0.366 (2.68)
MCI	−3.33 (3.12)	−5.49 (3.60)	−7.66 (3.59)
Median follow-up, years	4.02	3.39	3.49

Participants were stratified into clearly normal, intermediate range, and clearly abnormal groups with the hereby proposed three-range cut-points according to their CSF p-tau<sub>181</sub>/Aβ<sub>1-42</sub> levels measured with the Roche Elecsys immunoassay. The derived cut-points classified CSF p-tau<sub>181</sub>/Aβ<sub>1-42</sub> measurements as: <0.0203, clearly normal; ≥0.0203 and ≤0.0377, intermediate range; >0.0377, clearly abnormal. We observed, across the three-range abnormality spectrum, a trend for increases in age and number of APOE ε4 carriers and for decreases in cognitive composites for individuals with some level of impairment.

Abbreviations: ADNI, Alzheimer's Disease Neuroimaging Initiative; APOE ε4: apolipoprotein E ε4 allele; Aβ<sub>1-42</sub>, amyloid beta 1-42; CSF, cerebrospinal fluid; CU, cognitively unimpaired; MCI, mild cognitive impairment; MMSE, Mini-Mental State Examination; mPACC, modified Preclinical Alzheimer's Cognitive Composite.; p-tau<sub>181</sub>, tau phosphorylated at threonine-181; SD, standard deviation.

range cut-points (Figure 2D), the intermediate group presents significantly higher amyloid-PET levels in comparison to the clearly normal ( $P < .001$ ), and significantly lower in comparison to the clearly abnormal ( $P < .001$ ) group, revealing its capability of refining pathological stratification. For MCI individuals grouped with the binary cut-point (Figure 2E), biomarker-positive individuals presented significantly higher ( $P < .001$ ) amyloid-PET levels than biomarker-negative individuals. When grouping MCI individuals with the CSF three-range cut-points (Figure 2F), the intermediate group presented significantly higher amyloid PET levels than the clearly normal ( $P < .001$ ) and significantly lower than the clearly abnormal group ( $P < .001$ ).

In Figure 2G-J, raincloud plots demonstrate baseline differences in cognition (mPACC) between the CSF p-tau<sub>181</sub>/Aβ<sub>1-42</sub> biomarker groups. Although the three-range approach did not provide better stratification than dichotomization in cognition levels in CU individuals (Figure 2G-H), the three groups presented significant differences in cognition between each other in MCI individuals (Figure 2I-J).

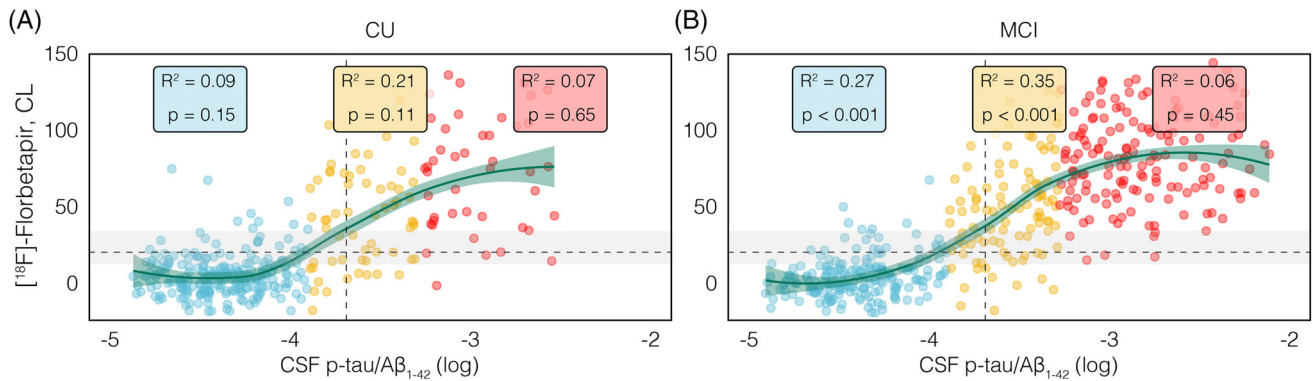
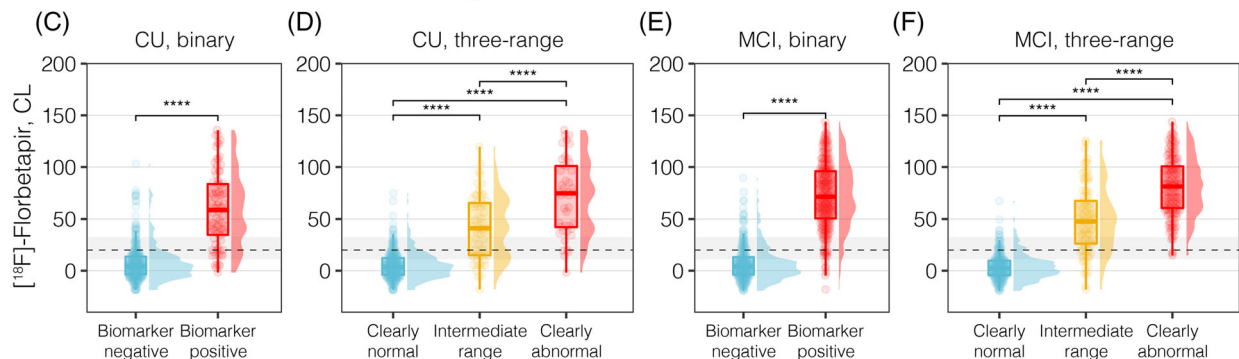
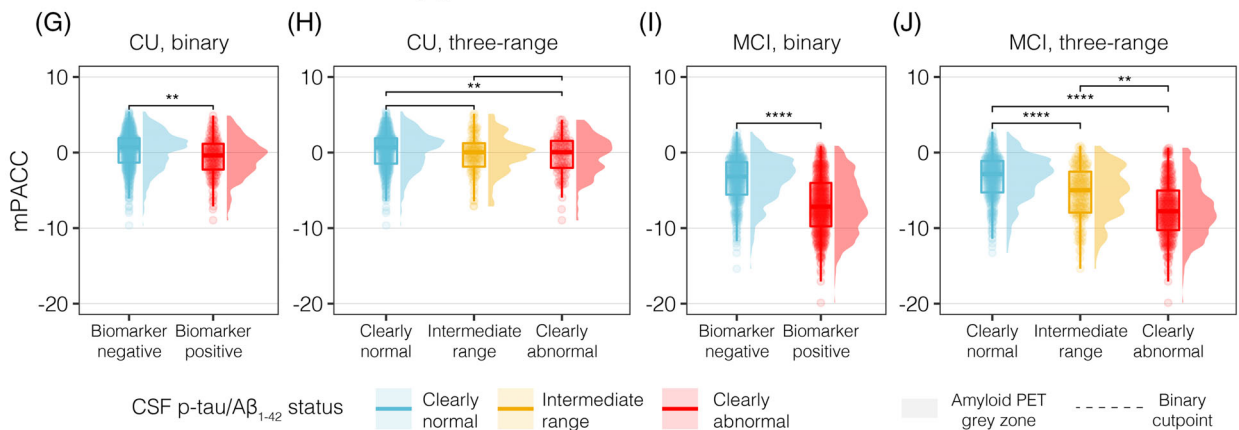
### 3.3 | Longitudinal cognitive trajectories

Based on baseline CSF p-tau<sub>181</sub>/Aβ<sub>1-42</sub> status, mean observed and predicted cognitive trajectories for the most common profile of covariates are shown in Figure 3. For longitudinal models based on the other CSF biomarkers and other reference schemes not included in the main text, see Figures S5 and S6.

For CU individuals, neither binary nor three-range models identified significant baseline cognitive differences (Figure 3A). With the binary cut-point, significantly greater rates of decline were observed for a biomarker-positive, compared to a biomarker-negative status

(Figure 3A; β-estimate: −0.42; 95% confidence interval (CI): −0.53, −0.21;  $P < .0001$ ), as described previously.<sup>15</sup> For the CU three-range model (Figure 3B), in comparison to the clearly normal group, the estimated rate of cognitive decline for the intermediate-range group was −0.15 (95% CI: −0.28, −0.04;  $P < .05$ ) and −0.59 (95% CI: −0.72, −0.38;  $P < .0001$ ) for the clearly abnormal group. When comparing the clearly abnormal group to the intermediate-range group, the estimated rate of decline was of −0.44 mPACC units per year (95% CI: −0.62, −0.29;  $P < .001$ ), indicating that the intermediate trajectory significantly diverges from those of the other two groups. The CU three-range model presented a slightly higher R<sup>2</sup> and lower AIC (R<sup>2</sup> 0.24; AIC 11234) than the binary model (R<sup>2</sup> 0.23; AIC 11244), indicating it better fits the data.

For MCI individuals, however, significantly different baseline cognition levels and rates of decline were detected by both binary and three-range models. The baseline mPACC difference between biomarker-negative and biomarker-positive groups was −2.91 (Figure 3C; 95% CI: −3.56, −2.38;  $P < .0001$ ). Regarding longitudinal trajectories, a significantly greater rate of decline was for MCI individuals with a biomarker-positive, compared to a biomarker-negative status (Figure 3C; β-estimate: −1.82; 95% CI: −2.28, −1.42;  $P < .0001$ ), as described previously.<sup>15,29</sup> For the three-range MCI model (Figure 3D), the baseline mPACC difference between intermediate-range biomarker status and clearly normal was −1.49 (95% CI: −2.34, −0.69;  $P < .01$ ), whereas the difference between clearly abnormal and clearly normal was −3.63 (95% CI: −4.36, −2.87;  $P < .0001$ ). Furthermore, a significant baseline difference of −2.14 (95% CI: −2.93, −1.35;  $P < .0001$ ) was observed between clearly abnormal and intermediate-range groups. Regarding longitudinal trajectories, the intermediate-range and clearly abnormal groups presented, respectively, estimated rates of decline of −0.85

Continuous associations between CSF p-tau/A $\beta_{1-42}$  with Amyloid-PETCSF p-tau/A $\beta_{1-42}$  three-range groups and Amyloid-PETCSF p-tau/A $\beta_{1-42}$  three-range groups and baseline cognition

CSF p-tau/A $\beta_{1-42}$  status: Clearly normal (blue), Intermediate range (yellow), Clearly abnormal (red). Amyloid PET grey zone (gray box), Binary cutpoint (dashed line).

**FIGURE 2** Cross-sectional associations with amyloid-PET and cognition. Continuous associations between CSF p-tau<sub>181</sub>/A $\beta_{1-42}$  and amyloid-PET measured with [<sup>18</sup>F]-florbetapir in the longitudinal sample of CU (A) and MCI (B) (n = 817). [<sup>18</sup>F]-florbetapir is represented on the y-axis with the centiloid scale, and CSF biomarker values are represented on the x-axis. Dots are colored based on their CSF three-range status and Spearman correlations are demonstrated for each group. The horizontal dashed line represents the >1.11 (20 CL) threshold for cerebral amyloidosis; the vertical line represents the binary cut-point of >0.0251, previously described for the CSF p-tau<sub>181</sub>/A $\beta_{1-42}$  ratio; the horizontal gray box represents the amyloid-PET gray zone (12-35CL) containing previously described thresholds. P-values come from Spearman correlation analyses. (C-F) Concentrations of amyloid-PET across CSF p-tau<sub>181</sub>/A $\beta_{1-42}$  three-range groups. The amyloid-PET cortical composite is displayed in centiloids on the y-axis, and on the x-axis, CSF biomarker groups are represented either in binary groups stratified with previously described binary thresholds or with the herein derived three-range CSF p-tau<sub>181</sub>/A $\beta_{1-42}$  cut-points, for both CU (C-D) and MCI (E-F). The horizontal dashed line represents the binary threshold for cerebral amyloidosis, and the horizontal gray box represents the amyloid-PET gray zone (12-35CL) containing previously described thresholds. (G-J) Baseline levels of global cognition across CSF p-tau<sub>181</sub>/A $\beta_{1-42}$  three-range groups. The mPACC scale is on the y-axis, with biomarker groups on the x-axis, either in binary groups stratified with previously described binary thresholds or with the herein derived three-range CSF p-tau<sub>181</sub>/A $\beta_{1-42}$  cut-points, for both CU (G-H) and MCI (I-J). CL, centiloid scale; CSF, cerebrospinal fluid; p-tau<sub>181</sub>, tau phosphorylated at threonine-181; A $\beta_{1-42}$ , amyloid beta 1-42; CU, cognitively unimpaired; MCI, mild cognitive impairment; mPACC, modified Preclinical Alzheimer's Cognitive Composite

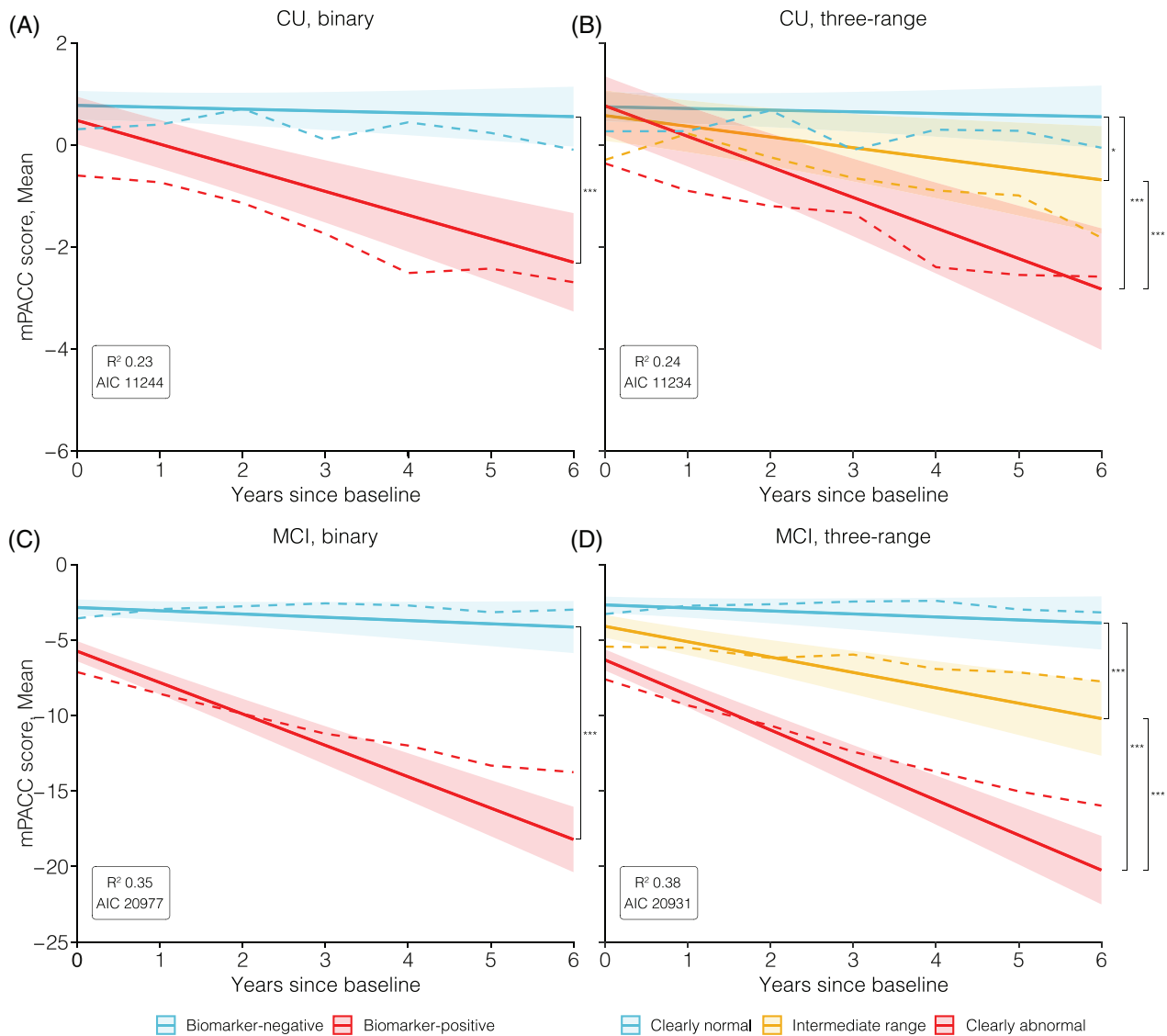


**FIGURE 3** Mean predicted cognitive trajectories according to binary and three-range CSF p-tau<sub>181</sub>/Aβ<sub>1-42</sub> cut-points. Mean observed (dashed colored line) and predicted (solid colored line) trajectories for the mPACC are displayed with 95% confidence intervals, according to the most common profile of covariates. Trajectories were estimated for a 6-year follow-up period including terms for CSF p-tau<sub>181</sub>/Aβ<sub>1-42</sub> biomarker group (binary or three-range), covariates (age, years of education, APOE ε4 status and sex), and their interactions with time. Mean cognitive trajectories are displayed for individuals CU at baseline according to binary (A) and three-range (B) status. For MCI individuals, mean cognitive trajectories are displayed according to binary (C) and three-range (D) biomarker groups, respectively. \*Asterisks represent *p*-values of the global slope comparison between the rates of decline (group-by-time interactions). The R<sup>2</sup>, a measure of how well the model explains outcome variability, and AIC, a goodness-of-fit metric, are displayed for each model in in-graph boxes. The previously described binary cut-point of 0.0251 was used for the CSF p-tau<sub>181</sub>/Aβ<sub>1-42</sub> ratio, whereas hereby derived cut-points of 0.0203 and 0.0377 were used for the three-range group. CSF, cerebrospinal fluid; p-tau<sub>181</sub>, tau phosphorylated at threonine-181; Aβ<sub>1-42</sub>, amyloid beta 1-42; APOE ε4, apolipoprotein E ε4 allele; CU, cognitively unimpaired; MCI, mild cognitive impairment; mPACC, modified Preclinical Alzheimer's Cognitive Composite; R<sup>2</sup>, coefficient of determination; AIC, Akaike information criterion

(95% CI: −1.08, −0.39; *P* < .001) and −2.05 (95% CI: −2.50, −1.67; *P* < .0001) in comparison to the clearly normal group. In comparison to the intermediate-range group, the clearly abnormal group also presented a significantly higher rate of cognitive decline, estimated as −1.20 (95% CI: −1.49, −0.74; *P* < .001) mPACC units per year. The MCI three-range model presented higher R<sup>2</sup> and lower AIC (R<sup>2</sup> 0.38; AIC 20977) than the binary model (R<sup>2</sup> 0.35; AIC 20931).

### 3.4 | Clinical progression

In Figure 4, Kaplan-Meier curves display the associations between baseline CSF p-tau<sub>181</sub>/Aβ<sub>1-42</sub> status and risk of clinical progression over a 6-year period.

In the CU-to-MCI binary model (Figure 4A), a biomarker-positive status for CSF p-tau<sub>181</sub>/Aβ<sub>1-42</sub> was associated with an increased risk



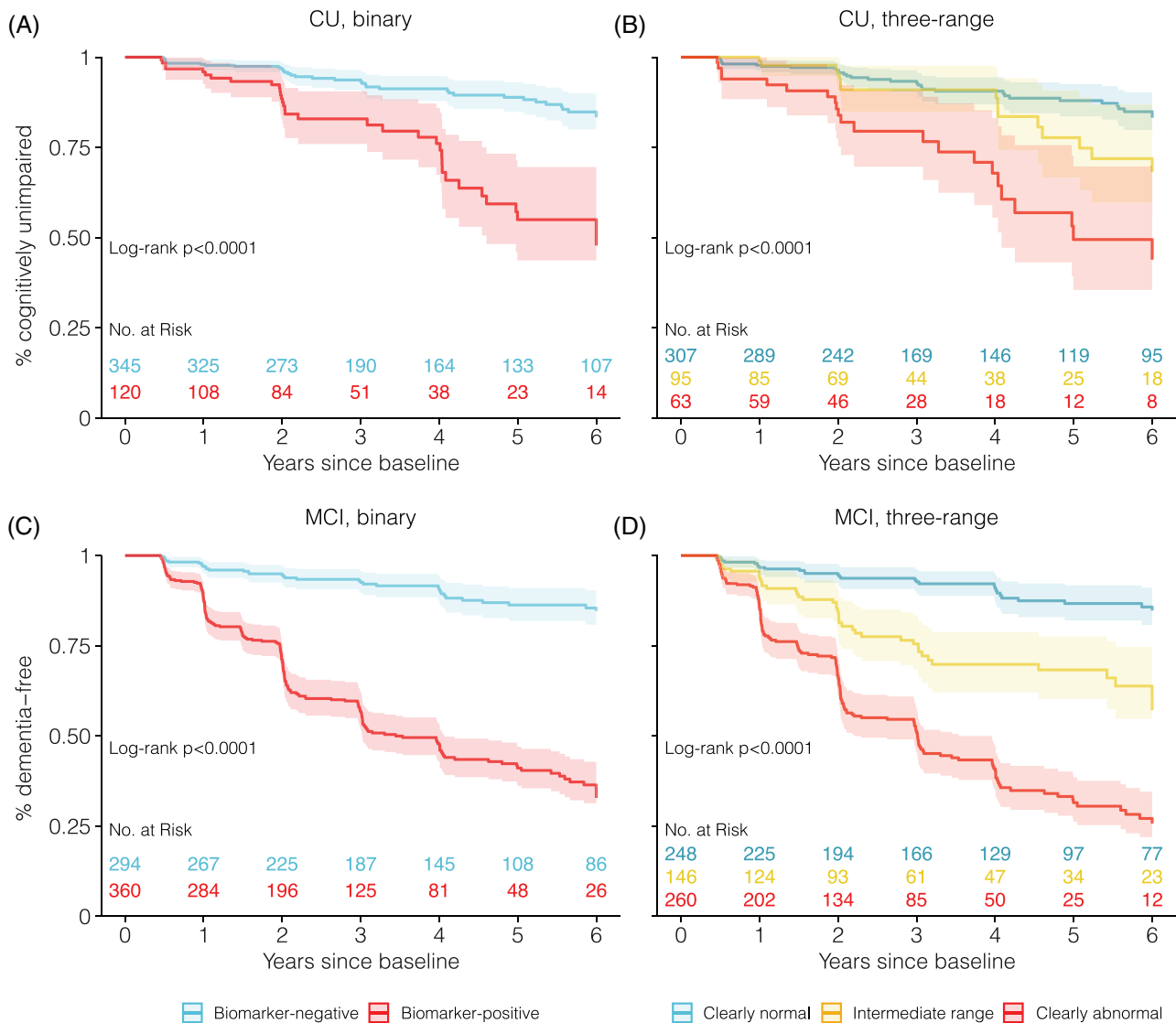


**FIGURE 4** Kaplan-Meier curves and the risk of onset of cognitive impairment or dementia according to binary and three-range CSF p-tau<sub>181</sub>/Aβ<sub>1-42</sub> cut-points. Kaplan-Meier curves for survival analysis predicting clinical progression according to CSF p-tau<sub>181</sub>/Aβ<sub>1-42</sub> baseline status. Survival curves are displayed for the conversion from CU to MCI according to binary (A) and three-range cut-points (B). For MCI to dementia, they are displayed according to binary (C) or three-range (D) biomarker status. The previously described binary cut-point of 0.0251 was used for CSF p-tau<sub>181</sub>/Aβ<sub>1-42</sub> ratio, whereas herein derived cut-points (0.0203; 0.0377) were used for the three-range group. CSF, cerebrospinal fluid; p-tau<sub>181</sub>, tau phosphorylated at threonine-181; Aβ<sub>1-42</sub>, amyloid beta 1-42; CU, cognitively unimpaired; MCI, mild cognitive impairment; mPACC, modified Preclinical Alzheimer's Cognitive Composite

of MCI onset for CU individuals (hazard ratio [HR] = 3.22, 95% CI: 1.84, 5.63;  $P < .0001$ ). In the CU-to-MCI three-range model (Figure 4B). Although an intermediate-range biomarker status was not associated with an elevated risk of cognitive impairment onset (HR = 1.57,  $P = .14$ , 95% CI: 0.84, 2.94,  $P = .13$ ), a significantly higher risk was observed for the clearly abnormal group (HR = 4.39, 95% CI: 2.30, 8.36;  $P < .0001$ ).

In the MCI-to-dementia binary model (Figure 4C), a biomarker-positive status for CSF p-tau<sub>181</sub>/Aβ<sub>1-42</sub> was associated with a greater risk of developing dementia for MCI individuals (Figure 4C; HR = 5.29; 95% CI: 3.53, 7.94;  $P < .0001$ ). In the three-range MCI-to-dementia model (Figure 4D), an intermediate-range status was significantly associated with an elevated risk of developing dementia (HR = 2.85, 95% CI:

1.70, 4.77;  $P < .0001$ ), with an even higher risk observed for the clearly abnormal group (HR = 5.76, 95% CI: 3.66, 9.05;  $P < .0001$ ).

### 3.5 | Power analysis

Based on a binary p-tau<sub>181</sub>/Aβ<sub>1-42</sub> cut-point, power analysis showed that 386 CU participants per arm (95% CI: 204, 1091) would be needed to detect a 25% reduction in rate of cognitive decline with 80% power in a trial lasting 48 months. Using the clearly abnormal cut-point for enrollment, we observed that only 199 participants per arm (95% CI: 111, 482) would be needed to obtain the same power. For MCI individ-

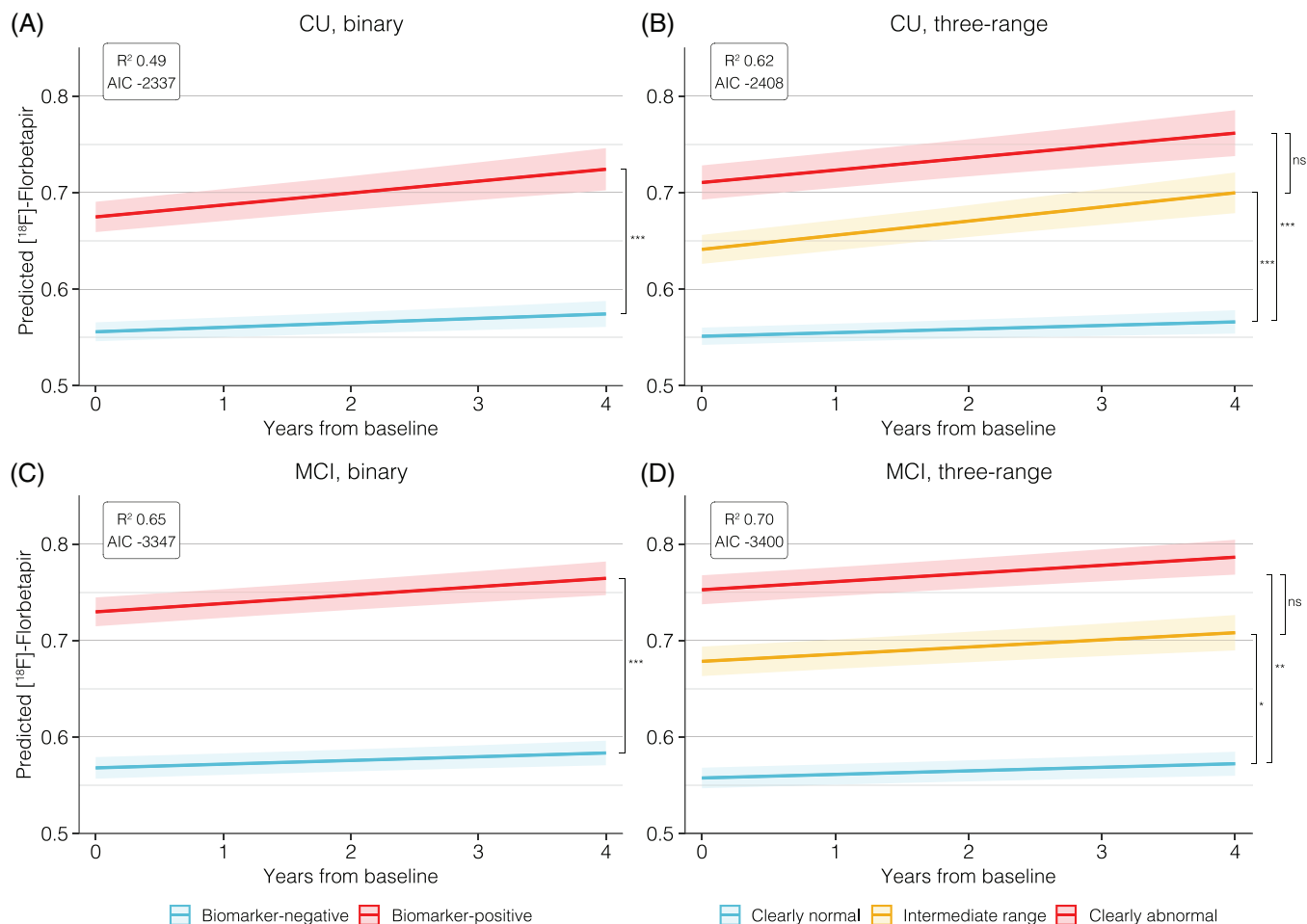


**FIGURE 5** Mean predicted trajectories of amyloid accumulation according to binary and three-range CSF p-tau<sub>181</sub>/A $\beta$ <sub>1-42</sub> cut-points. Mean predicted trajectories for the  $[^{18}\text{F}]$ -florbetapir longitudinal composite are displayed with 95% confidence intervals, according to the most common profile of covariates. Trajectories were estimated for a 4-year follow-up period including terms for CSF p-tau<sub>181</sub>/A $\beta$ <sub>1-42</sub> biomarker group (binary or three-range), covariates (age, years of education, APOE  $\epsilon$ 4 status, and sex), and their interactions with time. Mean amyloid-PET accumulation trajectories are displayed for individuals CU at baseline according to binary (A) and three-range (B) status. For MCI, amyloid-PET accumulation trajectories are displayed according to binary (C) and three-range (D) biomarker status. \*Asterisks represent  $p$ -values of the global slope comparison between the rates of decline (group-by-time interactions). The  $R^2$ , a measure of how well the model explains outcome variability, and AIC, a goodness-of-fit metric, are displayed for each model in in-graph boxes. The previously described binary cut-point of 0.0251 was used for CSF p-tau<sub>181</sub>/A $\beta$ <sub>1-42</sub> ratio, whereas hereby derived cut-points of 0.02033 and 0.0377 were used for the three-range group. The  $[^{18}\text{F}]$ -florbetapir composite normalized by subcortical eroded white matter was used, since it is recommended for longitudinal analyses. CSF, cerebrospinal fluid; p-tau<sub>181</sub>, tau phosphorylated at threonine-181; A $\beta$ <sub>1-42</sub>, amyloid beta 1-42; APOE  $\epsilon$ 4, apolipoprotein E  $\epsilon$ 4 allele; CU, cognitively unimpaired; MCI, mild cognitive impairment; mPACC, modified Preclinical Alzheimer's Cognitive Composite;  $R^2$ , coefficient of determination; AIC, Akaike Information Criterion

uals recruited based on the binary cut-point, 167 participants per arm (95% CI: 123, 242) would be needed to detect a 25% reduction in rate of cognitive decline, with 80% power in an 18-month trial. When using our more-stringent clearly abnormal classification for enrollment, 129 MCI participants per arm would be required (95% CI: 94, 188).

### 3.6 | Longitudinal amyloid accumulation

In Figure 5, we display predicted longitudinal trajectories of amyloid- $\beta$  deposition based on baseline CSF p-tau<sub>181</sub>/A $\beta$ <sub>1-42</sub> status. In line with our cross-sectional findings from Figure 2C-F, the binary and

three-range approach can detect significant baseline group differences. Figures S7 and S8 demonstrate trajectories for other biomarkers and cut-points.

In CU binary models (Figure 5A), a biomarker-positive status is associated with a higher yearly rate of A $\beta$  deposition in comparison to the biomarker-negative group ( $\beta$ -estimate: 0.0077; 95% CI: -0.004, 0.011;  $P < .001$ ). In CU three-range models (Figure 5B), the intermediate-range ( $\beta$ -estimate: 0.011; 95% CI: 0.007, 0.015;  $P < .001$ ) and the clearly abnormal ( $\beta$ -estimate: 0.009; 95% CI: 0.005, 0.013;  $P < .0001$ ) groups presented a significantly higher rate of A $\beta$  deposition in comparison to the clearly normal group, but not significantly differently between themselves ( $P = .48$ ). The CU three-range model presented

higher  $R^2$  and lower AIC ( $R^2$  0.62; AIC -2408) than the binary model ( $R^2$  0.49; AIC -2337).

In MCI binary models (Figure 5C), a biomarker-positive status is associated with a higher yearly rate of deposition in comparison to the biomarker-negative group ( $\beta$ -estimate: 0.005; 95% CI: -0.002, 0.007;  $P < .001$ ). In MCI three-range models (Figure 5D), the intermediate-range ( $\beta$ -estimate: 0.004; 95% CI: 0.002, 0.007;  $P < .05$ ) and the clearly abnormal ( $\beta$ -estimate: 0.005; 95% CI: 0.002, 0.008;  $P < .001$ ) groups presented a significantly higher rate of  $A\beta$  deposition in comparison to the clearly normal group, but not significantly differently between themselves ( $P = .51$ ). The MCI three-range model presented higher  $R^2$  and lower AIC ( $R^2$  0.65; AIC -3400) than the binary model ( $R^2$  0.70; AIC -3337).

## 4 | DISCUSSION

In this study, we derived three-range cut-points for CSF AD biomarkers and highlighted their application to the p-tau<sub>181</sub>/ $A\beta$ <sub>1-42</sub> ratio. Our longitudinal analyses demonstrated that this approach can reveal the existence of an intermediate cognitive trajectory undetected by dichotomization and identify faster-declining individuals, with power analyses demonstrating how this novel tool might be applied for population enrichment in clinical trials. Finally, we demonstrated that the CSF p-tau<sub>181</sub>/ $A\beta$ <sub>1-42</sub> three-range approach also identifies intermediate trajectories of  $A\beta$  deposition indexed by amyloid-PET.

As we enter the era of disease-modifying therapies, a growing vision among specialists<sup>36,37</sup> states that the recent approval is likely just an initial step toward finding effective therapies, as recently seen in other medical fields (eg, HIV drugs). In this context, developing tools for improving the next generation of clinical trials design is of utmost importance. Moreover, although there is a strong debate in the biomedical statistical community against dichotomization of biomarkers, clinical trial enrollment is one of the situations in which clear-cut decisions are often made in the AD field. In this context, handling enrollment biomarkers beyond dichotomization might be a valuable strategy, as recently seen in the donanemab trial.<sup>38</sup>

In this context, our longitudinal findings indicate that for prognostic assessment of CU and MCI individuals, expanding from dichotomization leads to the identification of a divergent intermediate cognitive trajectory and of a faster-declining clearly abnormal group. This applies not only for p-tau<sub>181</sub>/ $A\beta$ <sub>1-42</sub> but also for other evaluated CSF biomarkers (Figures S5 and S6). Previous studies focused either on discussing intermediate values in the context of amyloid-PET agreement<sup>9</sup> or in exploring the existence of an intermediate cognitive trajectory by grouping individuals based on descriptive statistics<sup>6,34,39</sup> (terciles, standard deviations, and so on), without having the objective of assessing prognostic value or of formally operationalizing a generalizable three-range approach.

In a more objective demonstration of the CSF three-range system utility in clinical trial design, our power analyses suggest that the three-range approach applied to CSF p-tau<sub>181</sub>/ $A\beta$ <sub>1-42</sub> could lead to smaller sample sizes needed for detecting cognitive decline for simulated clin-

ical trials with both CU and MCI individuals. In this scenario, the benefit would be due to recruiting clearly abnormal individuals, since they experience faster biomarker-related decline in comparison to those with a binary biomarker-positive status. We also showed how our approach can detect cross-sectional differences in amyloid-PET levels and global measures of cognition, which are important factors to consider when randomizing clinical trial intervention groups.

Furthermore, when modeling longitudinal trajectories of amyloid-PET deposition, we found that, for both CU and MCI groups, a CSF p-tau<sub>181</sub>/ $A\beta$ <sub>1-42</sub> intermediate-range status was associated with significantly faster rates in comparison to those of clearly normal individuals, but similar to that of clearly abnormal groups. These findings indicate that relevant pathophysiological information might go undetected by using binary CSF cut-points.

The methodology employed to define cut-points is a novel aspect in the AD fluid biomarkers literature. First, by defining an intermediate range for biomarker abnormality with TG-ROC, we avoided compromising specificity and sensitivity implicated by the usual "optimal" cut-point. Second, we demonstrate that reference schemes contrasting CU  $A\beta$ - with dementia  $A\beta$ + better captured a prognostically relevant CSF abnormality range for the p-tau<sub>181</sub>/ $A\beta$ <sub>1-42</sub>,<sup>16</sup> an emerging topic in the CSF biomarker debate, as proposed by Van Harten and colleagues.<sup>27</sup> In addition, the fully automated Elecsys immunoassay displays a very low inter-laboratory variability,<sup>16,40</sup> and the CSF p-tau<sub>181</sub>/ $A\beta$ <sub>1-42</sub> ratio seems even less sensitive to differences in pre-analytical handling than each biomarker alone,<sup>15,16</sup> which could favor their external validity. Given the current state of the AD field, we understand that this re-interpretation of the ROC method offers a potential interpretation trade-off between dichotomization and continuous-variable modeling, as it at least expands interpretation from a forced binary decision. Still, continuous modeling should be chosen whenever possible for extracting the most from biomarkers, and, in our opinion, future efforts should focus on a probabilistic interpretation of biomarkers in the context of a well-calibrated model including relevant covariates rather than discussing the addition of further categorization bins.

Although the focus of the present work resides in identifying a prognostically relevant CSF biomarker range with implications for trial enrollment and observational research, we understand it can also contribute to advancing the discussion on how fluid biomarkers should be interpreted in clinical practice. Contemporary understanding in medical decision-making theory argues that risk thresholds should be considered only when there is a decision to be made,<sup>41</sup> a more tangible notion to the AD field as novel disease-modifying treatments emerge. Considering a scenario in which CSF biomarkers are measured to consider administration of amyloid-targeting drugs, the presence or not of the proteinopathy would be the determinant factor—unlike our study, which exploratorily focused on clinico-biological prognostic assessment. For example, an individual with a high probability of having abnormal amyloid in the brain would be eligible for treatment; a patient with intermediate probability could be forwarded to amyloid-PET scanning if available, or, if not possible, have the CSF re-collected after a short period; a patient with low probability of having abnormal amyloidosis could have the CSF re-tested after a longer period

or, depending on symptoms, be forwarded to a differential diagnostic workup. However, we stress that this is the object of future work focusing on real-world clinical populations. The hereby derived cut-points are not fit for this purpose, but for advancing the research landscape on how to best handle fluid biomarkers, similarly to the ongoing research debate with the amyloid-PET gray zone. In fact, our findings are in line with amyloid-PET gray-zone studies, where intermediate burden is also associated with intermediate trajectories of cognitive decline and future amyloid deposition.<sup>7,8</sup>

Some limitations might affect the interpretation of our findings. The ADNI population consists of highly selected individuals, included based on willingness to participate in the study and on meeting specific enrollment criteria. Furthermore, it is a single-cohort study, and replication of the prognostic value of these ranges is warranted before external use. In addition, before being considered for trial recruitment, the impact of a clearly abnormal CSF cut-point over screening failure should be characterized. Future work should not only better elaborate the above-mentioned contexts of CSF biomarkers in decision-making, but should also aim at identifying individuals within the intermediate range that are at higher risk, potentially by incorporating relevant clinico-biological information in multidimensional models.

## ACKNOWLEDGMENTS

The authors would like to thank all the participants who volunteered to take part in the ADNI study, as well as the study leaders (acknowledged in the Appendix). They also thank Maude Wagner from Rush University for valuable methodological discussions and for providing help with the analyses, thank Giuliano Netto Flores Cruz from BiomeHub for critical reading of the manuscript and relevant discussions.

WSB is supported by the Coordination for the Improvement of Higher Education Personnel (CAPES) [88887.372371/2019-00] [88887.596742/2020-00]. MAB is supported by the National Council for Scientific and Technological Development (CNPq) [150293/2019-4]. AB is supported by CAPES [88882.345554/2019-01]. JPFS is supported by CAPES [88887.518039/2020-00]. DOS is supported by CNPq/INCT [465671/2014-4], CNPq/ZIKA [440763/2016-9], CNPq/FAPERGS/PRONEX [16/2551-0000475-7], FAPERGS [19/2551-0000700-0], CAPES [88887.507218/2020-00] [88887.507161/2020-00]. HZ is a Wallenberg Scholar supported by grants from the Swedish Research Council (#2018-02532), the European Research Council (#681712), Swedish State Support for Clinical Research (#ALFGBG-720931), the Alzheimer Drug Discovery Foundation (ADDF), USA (#201809-2016862), the AD Strategic Fund and the Alzheimer's Association (#ADSF-21-831376-C, #ADSF-21-831381-C and #ADSF-21-831377-C), the Olav Thon Foundation, the Erling-Persson Family Foundation, Stiftelsen för Gamla Tjänarinnor, Hjärnfonden, Sweden (#FO2019-0228), the European Union's Horizon 2020 research and innovation program under the Marie Skłodowska-Curie grant agreement No 860197 (MIRIADE), and the UK Dementia Research Institute at UCL. TKK was funded by the BrightFocus Foundation (#A2020812F), the International Society for Neurochemistry's Career Development Grant, the Swedish Alzheimer Foundation (Alzheimerfonden; #AF-930627), the Swedish Brain

Foundation (Hjärnfonden; #FO2020-0240), the Swedish Dementia Foundation (Demensförbundet), the Swedish Parkinson Foundation (Parkinsonfonden), Gamla Tjänarinnor Foundation, the Aina (Ann) Wallströms and Mary-Ann Sjöbloms Foundation, the Agneta Prytz-Folkes & Gösta Folkes Foundation (#2020-00124), the Gun and Bertil Stohnes Foundation, and the Anna Lisa and Brother Björns-son's Foundation. KB is supported by the Swedish Research Council (#2017-00915), the ADDF, USA (#RDAPB-201809-2016615), the Swedish Alzheimer Foundation (#AF-742881), Hjärnfonden, Sweden (#FO2017-0243), the Swedish State under the agreement between the Swedish government and the County Councils, the ALF-agreement (#ALFGBG-715986), the European Union Joint Program for Neurodegenerative Disorders (JPND2019-466-236), and the National Institutes of Health (NIH), USA, (grant #1R01AG068398-01). PRN and JT are supported by McGill University Faculty of Medicine, Alzheimer's Society of Canada, Alzheimer's Association, Weston Brain Institute, and Canadian Institutes of Health Research (CIHR). ERZ is supported by CNPq [435642/2018-9] and [312410/2018-2], Instituto Serrapilheira [Serra-1912-31365], Brazilian National Institute of Science and Technology in Excitotoxicity and Neuroprotection [465671/2014-4], FAPERGS/MS/CNPq/SESRS-PPSUS [30786.434.24734.23112017], the Alzheimer's Association [AARGD-21-850670] and ARD/FAPERGS [21/2551-0000673-0].

Data used in the preparation of this article were obtained from the Alzheimer's Disease Neuroimaging Initiative (ADNI) database ([adni.loni.usc.edu](http://adni.loni.usc.edu)).

## CONFLICTS OF INTEREST

HZ has served on scientific advisory boards for Eisai, Denali, Roche Diagnostics, Wave, Samumed, Siemens Healthineers, Pinteon Therapeutics, Nervgen, AZTherapies, and CogRx; and has given lectures in symposia sponsored by Cellectricon, Fujirebio, Alzecure, and Biogen. KB has served as a consultant, on advisory boards, or on data monitoring committees for Abcam, Axon, Biogen, JOMDD/Shimadzu, Julius Clinical, Lilly, MagQu, Novartis, Siemens Healthineers, and Roche Diagnostics. HZ and KB are co-founders of Brain Biomarker Solutions in Gothenburg AB, a GU Ventures-based platform company at the University of Gothenburg. The other authors declare no competing interests.

## AUTHOR CONTRIBUTIONS

Concept and design: WSB, MAB, AB, JT, JPFS, and ERZ. Acquisition, analysis, or interpretation of data: WSB, MAB, AB, JT, JPFS, PSC, TAP, TK, and ERZ. Drafting of the manuscript: WSB, MAB, AB, JT, JPFS, TK, and ERZ. Critical revision of the manuscript for important intellectual content: All authors. Statistical analysis: WSB, MAB, and PSC. Obtained funding: DOS and ERZ. Administrative, technical, or material support: DOS and ERZ. Supervision: ERZ.

## REFERENCES

1. Jack CR, Bennett DA, Blennow K, et al. NIA-AA Research Framework: toward a biological definition of Alzheimer's disease. *Alzheimer's Dement*. 2018; 14: 535-562.

2. Sperling RA, Aisen PS, Beckett LA, et al. Toward defining the preclinical stages of Alzheimer's disease: recommendations from the National Institute on Aging-Alzheimer's Association workgroups on diagnostic guidelines for Alzheimer's disease. *Alzheimer's Dement.* 2011; 7: 280-292.
3. Dubois B, Feldman HH, Jacova C, et al. Advancing research diagnostic criteria for Alzheimer's disease: the IWG-2 criteria. *Lancet Neurol.* 2014; 13: 614-629.
4. Barnes J, Bartlett JW, Fox NC, Schott JM. Targeted recruitment using cerebrospinal fluid biomarkers: implications for Alzheimer's disease therapeutic trials. *J Alzheimer's Dis.* 2013; 34: 431-437.
5. Grill JD, Nuño MM, Gillen DL. Which MCI patients should be included in prodromal Alzheimer disease clinical trials?. *Alzheimer Dis Assoc Disord.* 2019; 33: 104-112.
6. Mcrae-Mckee K, Udeh-Momoh CT, Price G, et al. Perspective: clinical relevance of the dichotomous classification of Alzheimer's disease biomarkers: should there be a "gray zone"?. *Alzheimer's Dement.* 2019; 15: 1348-1356.
7. Bullich S, Roé-Vellvé N, Marquí M, et al. Early detection of amyloid load using 18F-florbetaben PET. *Alzheimers Res Ther.* 2021; 13: 67.
8. Ebenau JL, Verfaillie SCJ, Van Den Bosch KA, et al. Grey zone amyloid burden affects memory function: the SCIENCe project. *Eur J Nucl Med Mol Imaging.* 2021; 48: 747-756.
9. Salvadó G, Molinuevo JL, Brugalat-Serrat A, et al. Centiloid cut-off values for optimal agreement between PET and CSF core AD biomarkers. *Alzheimers Res Ther.* 2019; 11: 27.
10. Ackley SF, Zimmerman SC, Brenowitz WD, et al. Effect of reductions in amyloid levels on cognitive change in randomized trials: instrumental variable meta-analysis. *BMJ.* 2021; 372: n156.
11. Harrell FE. *Regression Modeling Strategies.* Springer International Publishing; 2015. <https://doi.org/10.1007/978-3-319-19425-7>.
12. Petersen RC, Aisen PS, Beckett LA, et al. Alzheimer's Disease Neuroimaging Initiative (ADNI): clinical characterization. *Neurology.* 2010; 74: 201-209.
13. Bittner T, Zetterberg H, Teunissen CE, et al. Technical performance of a novel, fully automated electrochemiluminescence immunoassay for the quantitation of  $\beta$ -amyloid (1-42) in human cerebrospinal fluid. *Alzheimer's Dement.* 2016; 12: 517-526.
14. Lifke V, Kollmorgen G, Manuilova E, et al. Elecsys® Total-Tau and Phospho-Tau (181P) CSF assays: analytical performance of the novel, fully automated immunoassays for quantification of tau proteins in human cerebrospinal fluid. *Clin Biochem.* 2019; 72: 30-38.
15. Blennow K, Shaw LM, Stomrud E, et al. Predicting clinical decline and conversion to Alzheimer's disease or dementia using novel Elecsys A $\beta$ (1-42), pTau and tTau CSF immunoassays. *Sci Rep.* 2019; 9: 19024.
16. Hansson O, Seibyl J, Stomrud E, et al. CSF biomarkers of Alzheimer's disease concord with amyloid- $\beta$  PET and predict clinical progression: a study of fully automated immunoassays in BioFINDER and ADNI cohorts. *Alzheimer's Dement.* 2018; 14: 1470-1481.
17. Bates D, Mächler M, Bolker B, Walker S. Fitting linear mixed-effects models using lme4. *J Stat Softw.* 2015; 67.
18. Kassambara A, Kosinski M, Biecek P, *survminer: Drawing Survival Curves using 'ggplot2'.* R package version 0.4.8.999; 2020. <http://www.sthda.com/english/rpkgs/survminer/>
19. Anderson-Bergman C. icenReg: regression models for interval censored data in R. *J Stat Softw.* 2017; 81: 1-23.
20. Brasil P, DiagnosisMed: diagnostic test accuracy evaluation for health professionals. R package version 0.2.9.2/r58; 2018. <https://r-forge.r-project.org/projects/diagnosismed/>
21. Donohue MC, longpower: power and sample size calculations for longitudinal data. R package version 1.0-21; 2020. <https://cran.r-project.org/web/packages/longpower/>
22. Lüdecke D, sjPlot: data visualization for statistics in social science. R package version 2.8.6; 2020. <https://cran.r-project.org/package=sjPlot>
23. Lenth RV, emmeans: estimated marginal means, aka least-squares means. R package version 1.5.3; 2020.
24. Donohue MC, Sperling RA, Salmon DP, et al. The preclinical alzheimer cognitive composite. *JAMA Neurol.* 2014; 71: 961.
25. Royse SK, Minhas DS, Lopresti BJ, et al. Validation of amyloid PET positivity thresholds in centiloids: a multisite PET study approach. *Alzheimers Res Ther.* 2021; 13: 99.
26. Greiner M, Sohr D, Göbel P. A modified ROC analysis for the selection of cut-off values and the definition of intermediate results of serodiagnostic tests. *J Immunol Methods.* 1995; 185: 123-132.
27. Harten AC, Wiste HJ, Weigand SD, et al. Detection of Alzheimer's disease amyloid beta 1-42, p-tau, and t-tau assays. *Alzheimer's Dement.* 2021. <https://doi.org/10.1002/alz.12406>.
28. Wagner M, Helmer C, Tzourio C, Berr C, Proust-Lima C, Samieri C. Evaluation of the concurrent trajectories of cardiometabolic risk factors in the 14 years before dementia. *JAMA Psychiatry.* 2018; 75: 1033.
29. Jack CR, Wiste HJ, Therneau TM, et al. Associations of amyloid, tau, and neurodegeneration biomarker profiles with rates of memory decline among individuals without dementia. *JAMA.* 2019; 321: 2316.
30. Fitzmaurice GM, Laird NM, Ware JH. *Applied Longitudinal Analysis.* John Wiley & Sons, Inc.; 2011. <https://doi.org/10.1002/9781119513469>.
31. Zhao Yu, Edland SD. Power formulas for mixed effects models with random slope and intercept comparing rate of change across groups. *Int J Biostat.* 2021. <https://doi.org/10.1515/ijb-2020-0107>.
32. Ard MC, Edland SD. Power calculations for clinical trials in Alzheimer's disease. *J Alzheimer's Dis.* 2011; 26: 369-377.
33. Liu G, Liang K-Y. Sample size calculations for studies with correlated observations. *Biometrics.* 1997; 53: 937-947.
34. Mattsson-Carlgen N, Janelidze S, Palmqvist S, et al. Longitudinal plasma p-tau217 is increased in early stages of Alzheimer's disease. *Brain.* 2020; 143: 3234-3241.
35. Ingala S, De Boer C, Masselink LA, et al. Application of the ATN classification scheme in a population without dementia: findings from the EPAD cohort. *Alzheimer's Dement.* 2021. <https://doi.org/10.1002/alz.12292>.
36. Rabinovici GD. Controversy and progress in Alzheimer's disease – FDA approval of aducanumab. *N Engl J Med.* 2021; 385: 771-774.
37. Lalli G, Schott JM, Hardy J, De Strooper B. Aducanumab: a new phase in therapeutic development for Alzheimer's disease?. *EMBO Mol Med.* 2021; 13.
38. Mintun MA, Lo AC, Duggan Evans C, et al. Donanemab in early Alzheimer's disease. *N Engl J Med.* 2021. <https://doi.org/10.1056/NEJMoa2100708>.
39. Simrén J, Leuzy A, Karikari TK, et al. The diagnostic and prognostic capabilities of plasma biomarkers in Alzheimer's disease. *Alzheimer's Dement.* 2021. <https://doi.org/10.1002/alz.12283>.
40. Mattsson N, Andreasson U, Persson S, et al. CSF biomarker variability in the Alzheimer's Association quality control program. *Alzheimer's Dement.* 2013; 9: 251-261.
41. Vickers AJ, Elkin EB. Decision curve analysis: a novel method for evaluating prediction models. *Med Decis Mak.* 2006; 26: 565-574.

## SUPPORTING INFORMATION

Additional supporting information may be found in the online version of the article at the publisher's website.

**How to cite this article:** Brum WS, de Bastiani MA, Bieger A, et al. for the Alzheimer's Disease Neuroimaging Initiative (ADNI). A three-range approach enhances the prognostic utility of CSF biomarkers in Alzheimer's disease. *Alzheimer's Dement.* 2022;8:e12270. <https://doi.org/10.1002/trc2.12270>

## APPENDIX

### Collaborators

The investigators within the Alzheimer's Disease Neuroimaging Initiative (ADNI) contributed to the design and implementation of their study and/or provided data but did not participate in the analysis or writing of this report. A complete list of investigators and affiliations can be found at [http://adni.loni.usc.edu/wp-content/uploads/how\\_to\\_apply/ADNI\\_Acknowledgement\\_List.pdf](http://adni.loni.usc.edu/wp-content/uploads/how_to_apply/ADNI_Acknowledgement_List.pdf). The ADNI was launched in 2003 as a public-private partnership, led by principal investigator Michael W. Weiner, MD. Data collection and sharing for this project was funded by the ADNI (National Institutes of Health Grant U01 AG024904) and DOD ADNI (Department of Defense award number W81XWH-12-2-0012). ADNI is funded by the National Insti-

tute on Aging, the National Institute of Biomedical Imaging and Bioengineering, and through generous contributions from the following: AbbVie, Alzheimer's Association; Alzheimer's Drug Discovery Foundation; Araclon Biotech; BioClinica, Inc.; Biogen; Bristol-Myers Squibb Company; CereSpir, Inc.; Cogstate; Eisai Inc.; Elan Pharmaceuticals, Inc.; Eli Lilly and Company; EuroImmun; F. Hoffmann-La Roche Ltd and its affiliated company Genentech, Inc.; Fujirebio; GE Healthcare; IXICO Ltd.; Janssen Alzheimer Immunotherapy Research & Development, LLC.; Johnson & Johnson Pharmaceutical Research & Development LLC.; Lumosity; Lundbeck; Merck & Co., Inc.; Meso Scale Diagnostics, LLC.; NeuroRx Research; Neurotrack Technologies; Novartis Pharmaceuticals Corporation; Pfizer Inc.; Piramal Imaging; Servier; Takeda Pharmaceutical Company; and Transition Therapeutics. The Canadian Institutes of Health Research is providing funds to support ADNI clinical sites in Canada. Private sector contributions are facilitated by the Foundation for the National Institutes of Health ([www.fnih.org](http://www.fnih.org)). The grantee organization is the Northern California Institute for Research and Education, and the study is coordinated by the Alzheimer's Therapeutic Research Institute at the University of Southern California. ADNI data are disseminated by the Laboratory for Neuro Imaging at the University of Southern California.